Supporting Information for

Enhanced Polarization-sensitive Terahertz Emission from Vertical Grown Graphene by Dynamical Photon drag Effect

Lipeng Zhu[a], Yuanyuan Huang[a], Zehan Yao[a], Baogang Quan[b], Longhui Zhang [a], Junjie Li[b], Changzhi Gu[b], Xinlong Xu[a*], Zhaoyu Ren[a*]

[a] Shaanxi Joint Lab of Graphene, State Key Lab Incubation Base of Photoelectric Technology and Functional Materials, International Collaborative Center on Photoelectric Technology and Nano Functional Materials, Institute of Photonics & Photon-Technology, Northwest University, Xi'an 710069, China.

[b] Beijing National Laboratory for Condensed Matter Physics, and Institute of Physics, Chinese Academy of Sciences, Beijing 100190, China.

* Corresponding author. Fax: +86 29 88303336

E-mail address: xlxuphy@nwu.edu.cn (X. Xu) , rzy@nwu.edu.cn (Z. Ren)

1. Analysis of photoinduced current density in VGG

To simplify the model, we firstly consider the condition that one graphene nanoflake grown normal to the substrate as shown in Fig.S1. Then we can integrate the orientation angle γ to be consistent with the experiments. The photo-induced current density can be expressed as follows[1, 2],

$$\begin{aligned} \mathrm{j_i} &= \frac{i}{2} T_{ijkl} \{ \mathrm{E}_j (\nabla_l \mathrm{E}_k^*) - (\nabla_l \mathrm{E}_j) \mathrm{E}_k^* \} \\ &= \frac{i}{2} T_{ijkl} \{ -2\mathrm{i} \mathrm{k}_l \mathrm{E}_j \mathrm{E}_k^* \} \\ &= T_{ijkl} \, \mathrm{k}_l \mathrm{E}_j \mathrm{E}_k^* \end{aligned} \tag{S1}$$

Where T_{ijkl}, k, and *E* are fourth-rank tenser element, wave vector and electric field of the pump. As shown in Fig. S1, XYZ is laboratory coordinate system and xyz (the purple arrow) is crystal coordinate system. The subscript *i, j, k, l* represent the coordinate components of each physical quantity in crystal coordinate system xyz. Assuming that plane xy is in graphene surface and z axis perpendicular to the graphene plane (the gray plane), e.g. along the graphene normal direction. The XZ plane (the yellow plane) is the incident plane of the pump. The angles φ, θ are the polarization angle and incident angle of the pump beam respectively.

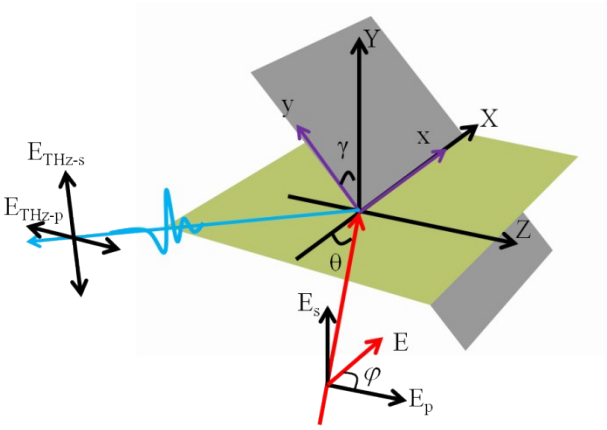

Fig. S1 Identification of polarization angles and Cartesian coordinate frame. φ is the incident polarization angle, θ is the incident angle and γ is the orientation angle.

Therefore the electrical vector projection of the pump beam in laboratory coordinate system can be presented as:

$$\begin{aligned} E_X &= E_p \sin\theta = E\cos\varphi\sin\theta \\ E_Y &= E_s = E\sin\varphi \\ E_Z &= E_p\cos\theta = E\cos\varphi\cos\theta \end{aligned} \tag{S2}$$

In crystal coordinate system, the electric vector can be gotten by rotating the laboratory coordinate along X axis for γ,

$$\begin{aligned} \begin{pmatrix} E_x \\ E_y \\ E_z \end{pmatrix} &= R_x(\gamma)\begin{pmatrix} E_X \\ E_Y \\ E_Z \end{pmatrix} \\ &= \begin{pmatrix} 1 & 0 & 0 \\ 0 & \cos\gamma & \sin\gamma \\ 0 & -\sin\gamma & \cos\gamma \end{pmatrix}\begin{pmatrix} E\cos\varphi\sin\theta \\ E\sin\varphi \\ E\cos\varphi\cos\theta \end{pmatrix} \\ &= \begin{pmatrix} E\cos\varphi\sin\theta \\ E\sin\varphi\cos\gamma + E\cos\varphi\cos\theta\sin\gamma \\ E\cos\varphi\cos\gamma\cos\theta - E\sin\varphi\sin\gamma \end{pmatrix} \end{aligned} \tag{S3}$$

Considering the graphene flakes vertically grown on substrate, its structure belongs to D_{6h} symmetry point group. *The nonzero elements of the fourth-rank T_{ijkl} are as follows* [3]:

$$\begin{aligned} &T_{zzzz}, \\ &T_{xxxx} = T_{yyyy} = T_{xxyy} + T_{xyxy} + T_{xyyx}, \\ &T_{xxyy} = T_{yyxx}, T_{xyxy} = T_{yxyx}, T_{xyyx} = T_{yxxy} \\ &T_{xxzz} = T_{yyzz}, T_{xzxz} = T_{yzyz}, T_{xzzx} = T_{yzzy} \\ &T_{zzxx} = T_{zzyy}, T_{zxzx} = T_{zyzy}, T_{zxxz} = T_{zyyz} \end{aligned} \tag{S4}$$

Considering the above nonzero elements, the x- and y-components current density j_x, j_y can be rewritten as :

$$\begin{aligned} j_x &= T_{xxxx}k_x E_x E_x^* + T_{xxzz}k_z E_x E_z^* + T_{xzxz}k_z E_z E_x^* \\ &\quad + T_{xzzx}k_x E_z E_z^* + T_{xyxy}k_y E_y E_x^* + T_{xxyy}k_y E_x E_y^* + T_{xyyx}k_x E_y E_y^* \\ &= T_{xyyx}(|E_x|^2 + |E_y|^2)k_x + 2T_{xxyy}(\mathrm{k}_x E_x^* + \mathrm{k}_y E_y^*)E_x \\ &\quad + T_{xzzx}k_x |E_z|^2 \end{aligned} \tag{S5}$$

$$
\begin{aligned}
j_y &= T_{yyyy} k_y E_y E_y^* + T_{yyzz} k_z E_y E_z^* + T_{yzyz} k_z E_z E_y^* \\
&\quad + T_{yzzy} k_y E_z E_z^* + T_{yxyx} k_x E_x E_y^* + T_{yyxx} k_x E_y E_x^* + T_{yxxy} k_y E_x E_x^* \\
&= T_{xyyx} (|E_x|^2 + |E_y|^2) k_y + 2T_{xxyy} (\mathrm{k}_y E_x^* + \mathrm{k}_x E_y^*) E_y \\
&\quad + T_{xzzx} k_y |E_z|^2
\end{aligned}
\tag{S6}
$$

Here the conditions $T_{ijkl} = T_{ikjl}$ are considered[1].

If the pump beam propagate in the XZ plane, the wave vector components in crystal coordinate frame are:

$$
\mathrm{k}_x = k \cos\theta \,, \quad \mathrm{k}_y = -k \sin\theta \sin\gamma \tag{S7}
$$

In terms of interband transition, in-plane carrier dominant, e.g. $|T_{\mathrm{xzzx}}| \ll |T_{\mathrm{xyyx}}|$

Applying all the above conditions, we can have:

$$
\begin{aligned}
j_x &= \mathrm{T}_{xyyx} k \cos\theta * \{(\mathrm{E}\cos\gamma \sin\varphi + \mathrm{E}\cos\varphi\cos\theta\sin\gamma)^2 + \mathrm{E}^2 \cos^2\varphi^2 \sin^2\theta\} \\
&\quad + \mathrm{T}_{xzzx} k \cos\theta (\mathrm{E}\sin\gamma\sin\varphi - \mathrm{E}\cos\gamma\cos\varphi\cos\theta)^2 \\
&\quad - 2E\, \mathrm{T}_{xxyy} \cos\varphi \sin\theta \{\mathrm{k}\sin\gamma\sin\theta(\mathrm{E}\cos\gamma\sin\varphi + E\cos\varphi\cos\theta * \sin\gamma) \\
&\quad - \mathrm{Ekcos}\varphi\cos\theta\sin\theta\}
\end{aligned}
\tag{S8}
$$

$$
\begin{aligned}
j_y &= -2\,\mathrm{T}_{xxyy} \{\mathrm{k}\sin\gamma\sin\theta(\mathrm{E}\cos\gamma\sin\varphi + E\cos\varphi\cos\theta\sin\gamma) \\
&\quad - \mathrm{Ekcos}\varphi\cos\theta\sin\theta\}(\mathrm{E}\cos\gamma\sin\varphi + E\cos\varphi\cos\theta\sin\gamma) \\
&\quad - \mathrm{T}_{xzzx} k \sin\gamma\sin\theta(\mathrm{E}\sin\gamma\sin\varphi - E\cos\gamma\cos\varphi\cos\theta)^2 \\
&\quad - T_{xyyx} k \sin\gamma\sin\theta\{(\mathrm{E}\cos\gamma\sin\varphi + E\cos\varphi\cos\theta\sin\gamma)^2 \\
&\quad + \mathrm{E}^2\cos^2\varphi\sin^2\theta\}
\end{aligned}
\tag{S9}
$$

So, the current density are:

$$
j_X = j_x \tag{S10}
$$

$$
j_Y = j_y \cos\gamma \tag{S11}
$$

$$
j_Z = j_y \sin\gamma \tag{S12}
$$

Integrate the variable γ from 0 to 2π for Equation (S11-S13)，we can get:

$$
\begin{aligned}
j_X &= \pi E^2 \mathrm{k}\cos\theta\{\mathrm{T}_{xyyx} + T_{xzzx} + 2T_{xxyy} \cos^2\varphi + \mathrm{T}_{xyyx}\cos^2\varphi - \mathrm{T}_{xzzx}\cos^2\varphi \\
&\quad - 2T_{xxyy} \cos^2\varphi\cos^2\theta - \mathrm{T}_{xyyx}\cos^2\varphi\cos^2\theta + T_{xzzx} \cos^2\varphi\cos^2\theta\} \\
&= \pi E^2 \mathrm{k}\cos\theta\cos^2\varphi\{2T_{xxyy} + \mathrm{T}_{xyyx} - \mathrm{T}_{xzzx} - 2T_{xxyy} \cos^2\theta - \mathrm{T}_{xyyx}\cos^2\theta \\
&\quad + T_{xzzx} \cos^2\theta\} + \pi E^2 \mathrm{k}\cos\theta(\mathrm{T}_{xyyx} + T_{xzzx})
\end{aligned}
\tag{S13}
$$

$$
\begin{aligned}
j_Y &= \frac{1}{2}\pi E^2 \,\mathrm{k}\cos\varphi\sin\varphi\cos\theta\sin\theta(2\,\mathrm{T}_{xxyy} - \mathrm{T}_{xyyx} + \mathrm{T}_{xzzx}) \\
&= \frac{1}{8}\pi E^2 \,\mathrm{k}\sin 2\varphi\sin 2\theta(2\,\mathrm{T}_{xxyy} - \mathrm{T}_{xyyx} + \mathrm{T}_{xzzx})
\end{aligned} \tag{S14}
$$

$$
\begin{aligned}
j_Z &= \frac{1}{2}\pi E^2 T_{xxyy}\, k\,\sin\theta - \frac{1}{2}\pi E^2 T_{xxyy}\, k\,\sin^3\theta - \pi E^2 T_{xxyy}\, k\,\sin^2\varphi\sin\theta \\
&\quad - \frac{1}{4}\{\pi E^2 T_{xyyx}\,\mathrm{k}\sin\theta(\sin^2\varphi + 3(\sin^2\varphi - 1)(\sin^2\theta - 1))\} + \\
&\quad \frac{1}{2}\pi E^2 T_{xxyy}\, k\,\sin^2\varphi\sin^3\theta - \frac{1}{4}\pi E^2 T_{xzzx}\, k\,\sin\theta\{3\sin^2\varphi + \\
&\quad (\sin^2\varphi - 1)(\sin^2\theta - 1)\} + \pi E^2 T_{xyyx}\, k\,\sin^3\theta(\sin^2\varphi - 1) \\
&= \pi E^2 k\,\sin^2\varphi\{-T_{xxyy}\,\sin\theta - \frac{1}{4}T_{xyyx}\,\sin\theta(3\sin^2\theta - 2) \\
&\quad + \frac{1}{2}T_{xxyy}\,\sin^3\theta - \frac{1}{4}T_{xzzx}\,\sin\theta(2 + \sin^2\theta) + T_{xyyx}\,\sin^3\theta\} \\
&\quad + \pi E^2 k\,\{\frac{1}{2}(\sin\theta - \sin^3\theta) - \frac{1}{4}T_{xyyx}\,\sin\theta(3 - 3\sin^2\theta) \\
&\quad - \frac{1}{4}T_{xzzx}\,\sin\theta(1 - \sin^2\theta) - T_{xyyx}\,\sin^3\theta\}
\end{aligned} \tag{S15}
$$

The transient current induced THz emission can be described by a model of dipole radiation[4]. The THz radiation inside the sample can be expressed as[5],

$$
E_{THz-p}^{in} \propto (\sin\theta_{in}\frac{\partial j_X}{\partial t} + \cos\theta_{in}\frac{\partial j_Z}{\partial t}) \tag{S16}
$$

$$
E_{THz-s}^{in} \propto \frac{\partial}{\partial t} j_Y \tag{S17}
$$

Here θ_{in} is radiation angle inside the medium and *n* is the refractive indices of VGG.

When the radiation outside the sample, Fresnel coefficients, t_p, t_s, at the interface should be considered and the output of the THz signals can be further expressed as:

$$
\begin{aligned}
E_{THz-p}^{out} &\propto t_p(\sin\theta_{in}\frac{\partial j_X}{\partial t} + \cos\theta_{in}\frac{\partial j_Z}{\partial t}) = \frac{2\sqrt{\varepsilon_2}\cos\theta_{in}}{\sqrt{\varepsilon_1}\cos\theta_{in} + \sqrt{\varepsilon_1}\cos\theta_{in}}(\sin\theta_{in}\frac{\partial j_X}{\partial t} + \cos\theta_{in}\frac{\partial j_Z}{\partial t}) \\
&= \frac{2\sqrt{\varepsilon_2 - \varepsilon_1\sin^2\theta_{\mathrm{det}}}}{\varepsilon_2\cos\theta_{\mathrm{det}} + \sqrt{\varepsilon_1}\sqrt{\varepsilon_2 - \varepsilon_1\sin^2\theta_{\mathrm{det}}}}(\sqrt{\varepsilon_1}\sin\theta_{\mathrm{det}}\frac{\partial j_X}{\partial t} + \sqrt{\varepsilon_2 - \varepsilon_1\sin^2\theta_{\mathrm{det}}}\frac{\partial j_Z}{\partial t})
\end{aligned} \tag{S18}
$$

$$
\begin{aligned}
E_{THz-s}^{out} &\propto t_s(\theta)\frac{\partial j_Y}{\partial t} = \frac{2\sqrt{\varepsilon_2}\cos\theta_{in}}{\sqrt{\varepsilon_2}\cos\theta_{in} + \sqrt{\varepsilon_1}\cos\theta_{in}}\frac{\partial j_Y}{\partial t} \\
&= \frac{2\sqrt{\varepsilon_2 - \varepsilon_1\sin^2\theta_{\mathrm{det}}}}{\sqrt{\varepsilon_2 - \varepsilon_1\sin^2\theta_{\mathrm{det}}} + \sqrt{\varepsilon_1}\cos\theta_{\mathrm{det}}}\frac{\partial j_Y}{\partial t}
\end{aligned} \tag{S19}
$$

where θ_{det} is the detection angle, $\sqrt{\varepsilon_1}\sin\theta_{\text{det}} = \sqrt{\varepsilon_2}\sin\theta_{in}$, and ε_1 and ε_2 is the dielectric function in air and VGG medium.

2. VGG THz emission dependence on incident polarization angle

For reflection configuration, $\theta_{\text{det}} = 45°$, $\theta = 45°$. Therefore, $j_X \propto A\cos^2\varphi$+B, $j_Y \propto A^{''}\sin 2\varphi$, $j_Z \propto A^{'''}\sin^2\varphi + B^{'}$

$$E_{THz-p}^{out} \propto \frac{2\sqrt{\varepsilon_2 - \frac{1}{2}}}{\varepsilon_2\frac{\sqrt{2}}{2} + \sqrt{\varepsilon_2 - \frac{1}{2}}}\left(\frac{\sqrt{2}}{2}\frac{\partial j_X}{\partial t} + \sqrt{\varepsilon_2 - \frac{1}{2}}\frac{\partial j_Z}{\partial t}\right) \propto C\cos^2\varphi + D\sin^2\varphi + E \tag{S20}$$

$$E_{THz-s}^{out} \propto \frac{2\sqrt{\varepsilon_2 - \frac{1}{2}}}{\sqrt{\varepsilon_2 - \frac{1}{2}} + \frac{\sqrt{2}}{2}}\frac{\partial j_Y}{\partial t} \propto F\sin 2\varphi \tag{S21}$$

For transmission configuration, $\theta_{\text{det}} = 135°$, $\theta = 45°$.

$$E_{THz-p}^{out} \propto C^{'}\cos^2\varphi + D^{'}\sin^2\varphi + E^{'} \tag{S22}$$

$$E_{THz-s}^{out} \propto F^{'}\sin 2\varphi \tag{S23}$$

3. VGG THz emission dependence on incident angle

For transmission configuration, $\varphi = 15°$ and $\theta_{\text{det}} = \theta$.

thus, $j_X \propto A_1\cos\theta + B_1\cos^3\theta$, $j_Y \propto A_2\sin 2\theta$, $j_Z \propto A_3\sin\theta + B_3\sin^3\theta$

$$\begin{aligned} E_{THz-p}^{out} &\propto \frac{2\sqrt{\varepsilon_2 - \sin^2\theta}}{\varepsilon_2\cos\theta + \sqrt{\varepsilon_2 - \sin^2\theta}}\left(\sin\theta\frac{\partial j_X}{\partial t} + \sqrt{\varepsilon_2 - \sin^2\theta}\frac{\partial j_Z}{\partial t}\right) \\ &\propto \frac{2\sqrt{\varepsilon_2 - \sin^2\theta}}{\varepsilon_2\cos\theta + \sqrt{\varepsilon_2 - \sin^2\theta}}\{A_1\sin\theta\cos\theta + A_3\sqrt{\varepsilon_2 - \sin^2\theta}\sin\theta\} \end{aligned} \tag{S24}$$

Here, we ignore the small terms such as $\cos^3\theta$ and $\sin^3\theta$ as the coefficients A, B are nearly equal.

$$E_{THz-s}^{out} \propto \frac{2\sqrt{\varepsilon_2 - \sin^2\theta}}{\sqrt{\varepsilon_2 - \sin^2\theta} + \cos\theta}\frac{\partial j_Y}{\partial t} \propto A_2\frac{2\sqrt{\varepsilon_2 - \sin^2\theta}}{\sqrt{\varepsilon_2 - \sin^2\theta} + \cos\theta}\sin 2\theta \tag{S25}$$

4. Penetration depth of VGG at 800 nm

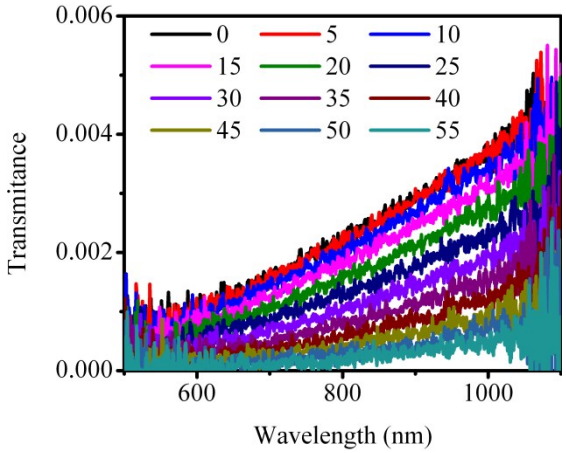

Fig. S2 Transmission spectroscopy of VGG at different incident angles.

In terms of the penetration depth of the 800 nm pump on VGG, we can estimate the value from the transmission spectroscopy of VGG shown in Fig. S2. The penetration depth at 800nm can be estimated by,

$$T = \frac{I}{I_0} = e^{-\alpha L}$$

Here α is absorption coefficient and L is sample thickness. When taking T=0.0025 and L=2 μm into consideration, we can calculate the penetration depth $d=1/\alpha=0.328\ \mu m^{-1}$ at 800 nm.

5. Raman spectroscopy characterization of single layer graphene

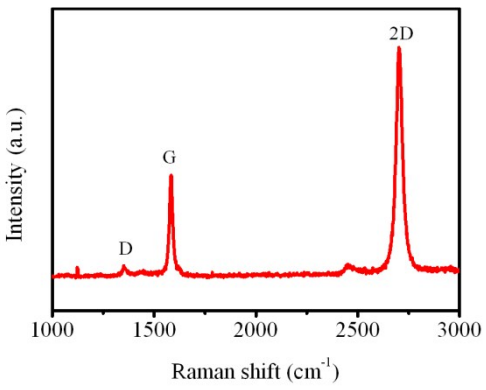

Fig. S3. Raman spectroscopy of single layer graphene excited by a 514 nm wavelength pulse.

Raman spectroscopy is used to identify the layer of the graphene as shown in Fig. S3. The weak D peak at 1351 cm^{-1} caused by the breathing modes of six-atom rings proves a low number of defects in graphene. The G peak at 1583 cm^{-1} due to E_{2g} phonon mode. And a single sharp 2D

peak at 2701 cm^{-1} owing to the second order of zone-boundary phonons illustrates that the graphene we used is a single layer graphene[6].

6. THz peak-valley value VS. spectrum area

In order to check that the method of using THz peak-valley value, we repeated the polarization angle dependent THz signals data via reflection configuration as shown in Fig. S4. Fig. S4(a) and (b) are polarization angle dependence of the THz peak-valley value for both p- (a) and s-polarization (b) in our manuscript. While Fig. S4(c) and (d) used spectrum area to represent THz signal for p- (c) and s-polarization (d). It is clear that the two methods show the same variation trend for both THz p- and s-components, which demonstrates that THz peak-valley value used in our manuscript is appropriate.

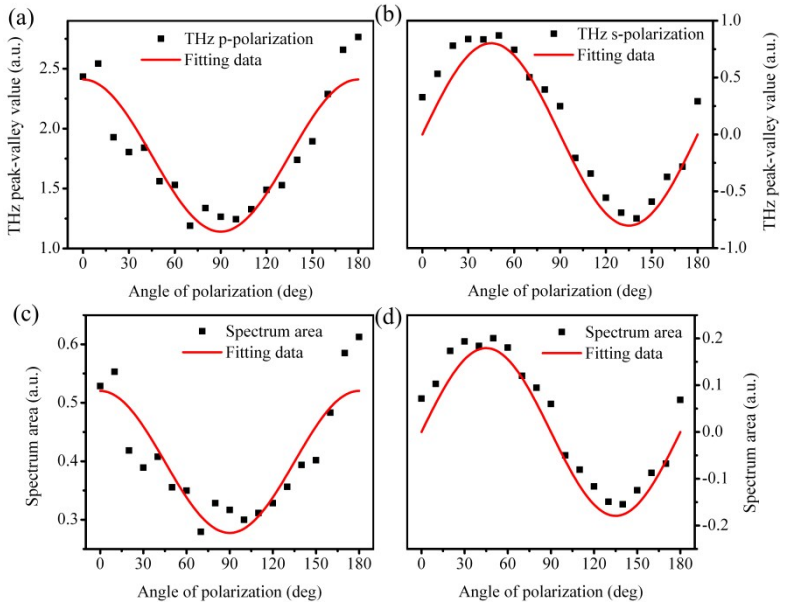

Fig. S4 THz signal changes with the polarization angle. The polarization angle dependence of THz peak-valley value for p- (a) and s-polarization (b). The polarization angle dependence of THz spectrum area for p- (c) and s-polarization (d).

Reference

1. P. A. Obraztsov, N. Kanda, K. Konishi, M. Kuwata-Gonokami, S. V. Garnov, A. N. Obraztsov and Y. P. Svirko, *Physical Review B*, 2014, **90**, 241416.
2. P. A. Obraztsov, T. Kaplas, S. V. Garnov, M. Kuwata-Gonokami, A. N. Obraztsov and Y. P. Svirko, *Scientific reports*, 2014, **4**, 4007.
3. R. W. Boyd, *Nonlinear Optics, Third Edition*, Academic Press, 2008.
4. X. C. Zhang and D. H. Auston, *Journal of Applied Physics*, 1992, **71**, 326-338.
5. M. B. Johnston, D. M. Whittaker, A. Corchia, A. G. Davies and E. H. Linfield, *Journal of Applied Physics*, 2002, **91**, 2104.
6. A. C. Ferrari, J. C. Meyer, V. Scardaci, C. Casiraghi, M. Lazzeri, F. Mauri, S. Piscanec, D. Jiang, K. S. Novoselov, S. Roth and A. K. Geim, *Phys Rev Lett*, 2006, **97**, 187401.